Calculation and interpretation of the continuum radiation of hydrogen molecules

U Fantz†, B Schalk†§ and K Behringer†‡

† Lehrstuhl für Experimentelle Plasmaphysik, Institut für Physik, Universität Augsburg, Universitätsstrasse 1, D-86135 Augsburg, Germany
‡ Max-Planck-Institut für Plasmaphysik, EURATOM Association, Boltzmannstrasse 2, D-85748 Garching, Germany
§ Present address: OSRAM GmbH, Hellabrunner Strasse 1, D-81536 München, Germany
E-mail: fantz@physik.uni-augsburg.de

Abstract. Calculations of the hydrogen molecular continuum ($a^3\Sigma_g^+ \rightarrow b^3\Sigma_u^+$, where the latter is repulsive) have been carried out in the wavelength range 120–600 nm, based on potential curves and reduced masses. They give transition probabilities, lifetimes and spectral intensities as a function of vibrational level population in the upper state $a^3\Sigma_g^+$. Absolute radiation measurements in H_2/He and D_2/He low-pressure ECR plasmas in the wavelength range 170–300 nm are compared with results from these calculations. Using the Franck–Condon principle and the corona model for excitation, the relative vibrational population in the upper state is correlated with the population in the ground state, characterized by the vibrational temperature T_{vib}. The absolute intensities depend on the electron temperature T_e via the electron excitation rate coefficients. Therefore, the shape of the continuum radiation reflects T_{vib}, and the absolute value is a function of T_e. The results are in good agreement with those from other spectroscopic techniques (T_e from He line intensities, T_{vib} from Fulcher band radiation) in the visible spectral range. This demonstrates that emission spectroscopy of the continuum radiation of H_2 and D_2 is a good tool for diagnostics of low-pressure plasmas. The calculations have also been carried out for other hydrogen isotopes (T_2, HD, DT).

1. Introduction

The continuum radiation of deuterium and hydrogen low-pressure arcs is commonly used as a standard calibration source in the UV spectral range. In low-pressure plasmas, hydrogen is often

present for producing and optimizing thin films. Emission spectroscopy in the visible range is frequently applied as a diagnostic method for the determination of plasma parameters, due to the low cost of the apparatus and its easy handling.

With respect to hydrogen molecules, rotational temperatures, vibrational populations and n_{H_2} can be derived from the emission of the Fulcher bands around 600 nm ($d^3\Pi_u \to a^3\Sigma_g^+$) [1–4]. The ratio of Balmer lines to Fulcher emission is used for determination of the degree of dissociation [3]. Due to the small masses involved, the Fulcher spectrum is a multiline spectrum and the vibrational bands and rotational lines frequently overlap. In contrast, the continuum radiation between 165 and 400 nm includes all vibrational transitions, has no overlapping lines and is reasonably intense. Calculations of radiation for this wavelength range were carried out in [5–7] with low energy or wavelength resolution, and only for relative intensities. Precise absolute calculations for H_2 are given in [8], including higher vibrational levels in $a^3\Sigma_g^+$. Comparisons with experimental data from electron beam measurements are presented, which concentrate on the emission spectrum from $v = 0$ in $a^3\Sigma_g^+$. Recently, comparisons of calculations and measurements in a capillary arc and various microwave plasmas have been reported [7]. The determination of T_{vib} in the ground state from this radiation was based on measurements of the relative intensities at two wavelengths with a high signal-to-noise ratio. However, this method is rather insensitive. In addition, the microwave plasmas contained argon, resulting in an overlapping continuum due to ArH^+ molecules. The calculations were carried out on a relative scale with a wavelength resolution of 5 nm and interpolation between the points. Measurements were carried out in the range 220–400 nm, without absolute calibration of the system.

In this paper, calculations of transition probabilities, lifetimes and radiation intensities are reported, with high resolutions for the whole wavelength range 120–600 nm on an absolute scale. The continuum was calculated for hydrogen molecules and their isotopes, as described in section 2. In the next section, the experiment and the absolute intensity measurements are presented. Section 4 gives a comparison of measurements and calculations, including a discussion of sensitivity. The results for T_{vib} and T_e are compared with the results of the analysis of the Fulcher band emission and He line emission, respectively, for H_2 and D_2. We conclude with calculations for other molecular hydrogen isotopes (T_2, HD, DT).

2. Calculation of the continuum radiation

The spectral photon emission coefficient of the bound–free transition $a^3\Sigma_g^+ \to b^3\Sigma_u^+$ is given by

$$I_\lambda(\lambda)\mathrm{d}\lambda = \sum_{v_a=0}^{\infty} n_{v_a} A_{v_a,\lambda}(\lambda)\mathrm{d}\lambda. \tag{1}$$

n_{v_a} is the population of the vibrational level v_a in $a^3\Sigma_g^+$, and $A_{v_a,\lambda}(\lambda)$ is the spectral transition probability from v_a. The latter is given by

$$A_{v_a,\lambda}(\lambda) = \frac{128\pi^3 c}{12\epsilon_0 h\lambda^5}\sqrt{\frac{2m_r}{E}}\left|\int_0^\infty \tilde{\psi}_E^*(r)D_{el}(r)\psi_{v_a}(r)\mathrm{d}r\right|^2 \tag{2}$$

where $\tilde{\psi}_E^*(r)$ is the vibrational wave function for $b^3\Sigma_u^+$ and energies E above the dissociation limit (figure 1). The amplitude is normalized to one at $r \to \infty$. $\psi_{v_a}(r)$ is the vibrational eigenfunction for the v_a level in the $a^3\Sigma_g^+$ state. In the vibrational wave functions, the rotational levels were averaged. Starting from the potential curves of the states involved, and the reduced mass m_r of
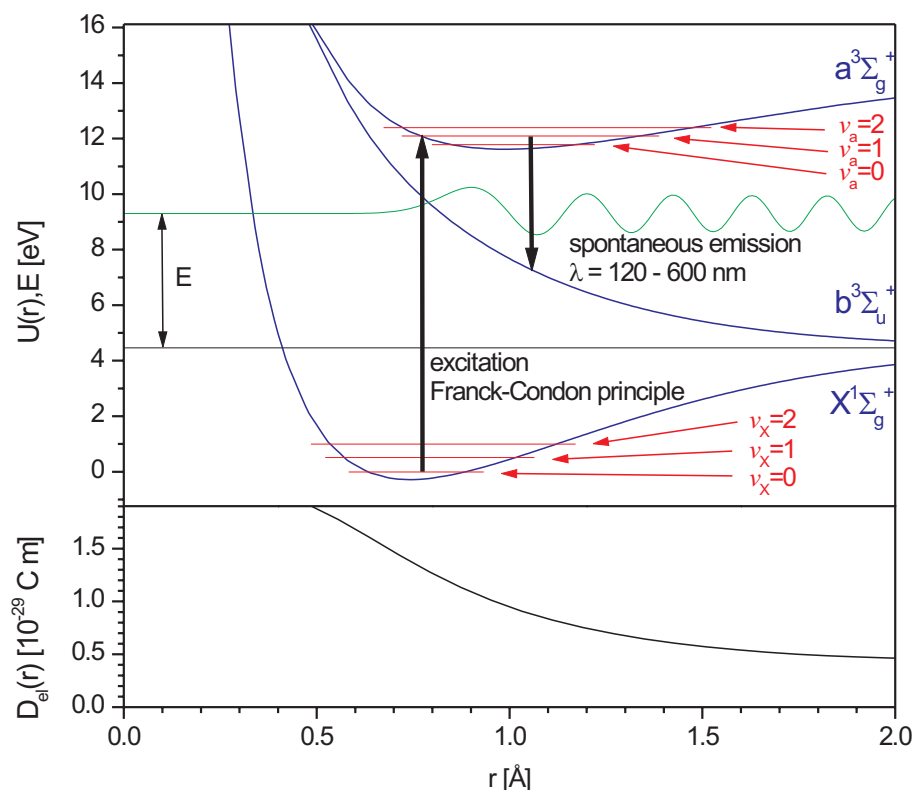
Figure 1. In the upper panel, the potential curves of $a^3\Sigma_g^+$ and $b^3\Sigma_u^+$ are shown together with the potential curve of the ground state, $X^1\Sigma_g^+$. The first three eigenvalues of the bound states are included. The lower panel shows the electronic transition dipole moment $D_{el}(r)$, taken from [8].

the molecule under consideration, the wave functions and eigenvalues can be calculated. The numerical procedures used will be discussed below. The potential curves (figure 1) were taken from the literature: those for $X^1\Sigma_g^+$ and $b^3\Sigma_u^+$ are from [9], and the curve for $a^3\Sigma_g^+$ is from [10]. They were calculated using the Born–Oppenheimer approximation, which may not be very well fulfilled for hydrogen molecules because of their small mass. The electronic transition dipole moment $D_{el}(r)$ was obtained by cubic spline interpolation between the data points from [8], and by using the fit formula given there for $r > 13a_0$. $D_{el}(r)$ is also plotted in figure 1. Note the variation in the relevant r range. The assumption of a constant D_{el} would not be justified.

Low-density plasmas are always far from thermodynamic equilibrium and a Boltzmann population of excited levels is not given. For the calculation of the populations n_{v_a} in the excited state, the corona model was used. Here, excitation from vibrational levels in the ground state $X^1\Sigma_g^+$ to the $a^3\Sigma_g^+$ state is balanced by spontaneous emission to $b^3\Sigma_u^+$:

$$n_{v_a} = \frac{\sum_{v_X=0}^{v_{X,max}} X_{v_X \to v_a}(T_e) n_{v_X} n_e}{A_{v_a}}. \tag{3}$$

A_{v_a} denotes the transition probability integrated over all wavelengths:

$$A_{v_a} = \int_0^\infty A_{v_a,\lambda}(\lambda)\mathrm{d}\lambda \tag{4}$$

n_{v_X} is the particle density in the vibrational state v_X in $X^1\Sigma_g^+$, n_e the electron density, and T_e the electron temperature. For the transition $X^1\Sigma_g^+ \to a^3\Sigma_g^+$, the cross-section for hydrogen from $v_X = 0$ to the sum of all vibrational levels in $a^3\Sigma_g^+$ can be found in [11–13], based on theoretical work. Measured data are scarce, however, three points at the higher energies 30, 50 and 70 eV are given in [14], which are in good agreement with the theoretical values. Discrepancies exist in the energy range below 30 eV, where [12] gives values which are a factor of two lower at the maximum of the cross-section than the data from other groups. An overview can be found in [15]. For this work, the cross-sections from [11] were chosen, because they represent the latest data with most data points, especially near the threshold energy. This becomes important for the low-temperature plasmas investigated here. For deuterium, the hydrogen cross-sections were applied. The excitation rate coefficient $X_0(T_e)$ from $v_X = 0$ to the sum of all vibrational states in $a^3\Sigma_g^+$ was then calculated by integrating these cross-sections over a Maxwellian distribution function for the electron energies. The vibrationally resolved excitation rate coefficients $X_{v_X \to v_a}(T_e)$ were derived from $X_0(T_e)$ using the Franck–Condon principle for excitation:

$$X_{v_X \to v_a}(T_e) = X_0(T_e)F(v_a, v_X)f_{v_X}^{vib}(T_e). \tag{5}$$

$f_{v_X}^{vib}(T_e)$ is an approximation for the reduced threshold energy. This factor was determined by decreasing the threshold energy of the cross-section by the difference of the eigenvalues of the vibrational states v_X and $v_X = 0$ in $X^1\Sigma_g^+$ in the integration. This correction becomes important for $T_e < 3$ eV and reaches values of about two. $F(v_a, v_X)$ are the Franck–Condon factors for the transitions from v_a in $a^3\Sigma_g^+$ to v_X in $X^1\Sigma_g^+$. For H_2, the Franck–Condon factors from $v_a = 0$–9 to $v_X = 0$ are listed in [14] and from $v_a = 0$–6 to $v_X = 0$–6 in [7]. Because of a lack of data for higher vibrational levels and for the hydrogen isotopes, the complete set of Franck–Condon factors was recalculated for $v_a = 0$–14 to $v_X = 0$–9 using:

$$F(v_a, v_X) = \left| \int_0^\infty \psi_{v_a}^*(r)\psi_{v_X}(r)\mathrm{d}r \right|^2. \tag{6}$$

Here, $\psi_{v_a}(r)$ denotes the vibrational wave function for v_a, and $\psi_{v_X}(r)$ is the vibrational wave function for v_X. The results for H_2 and D_2 are listed in tables 1 and 2, and the agreement for H_2 with the literature quoted above is very good.

The vibrational wave functions were obtained by solving the one-dimensional Schrödinger equation with the Taylor method of order three, starting with an arbitrary value for $\psi(0)$ and $\frac{\mathrm{d}\psi}{\mathrm{d}r}(0) = 0$ at $r = 0$ and a step size of 0.0001 Å for $0 < r < 10$ Å.

To find the eigenvalues, an iteration procedure was used, based on counting the number of zeros in the wave function for a given energy E. If E is below E_i (the energy of the eigenvalue of the vibrational level i in the examined state), then the number of zeros is lower than or equal to i. If E is above E_i, the number of zeros is greater than i. By starting with a given step size for the energy and going through several iterations, each time reducing the step size, the eigenvalues can be determined with arbitrary precision. For this work, the precision used was 0.001 cm^{-1}.

The methods presented here for calculating wave functions, eigenvalues, Franck–Condon factors and transition probabilities is generally applicable to all transitions in diatomic molecules.

Table 1. Franck–Condon factors for the transition $a^3\Sigma_g^+ \leftarrow X^1\Sigma_g^+$ for H_2. Tables of the Franck–Condon factors for all isotopes of the hydrogen molecule are available in ASCII format—click here.

v_a	$v_X = 0$	$v_X = 1$	$v_X = 2$	$v_X = 3$	$v_X = 4$
0	0.206612	0.401581	0.283780	0.092938	0.014184
1	0.254182	0.064944	0.083658	0.326811	0.217069
2	0.202859	0.005021	0.164152	0.002684	0.208100
3	0.134710	0.060123	0.051202	0.082317	0.071728
4	0.082145	0.094308	0.000523	0.100711	0.007112
5	0.048667	0.095056	0.014743	0.042507	0.066059
6	0.028274	0.078478	0.040493	0.004737	0.070189
7	0.016374	0.058303	0.053828	0.001734	0.036514
8	0.009704	0.041709	0.055468	0.013448	0.009775
9	0.005669	0.028158	0.048112	0.024087	0.000299
10	0.003492	0.019453	0.039932	0.030056	0.001814
11	0.002078	0.012670	0.029799	0.029118	0.006236
12	0.001292	0.008454	0.022015	0.025715	0.009536
13	0.000760	0.005237	0.014652	0.019269	0.009602
14	0.000380	0.002708	0.007938	0.011241	0.006606

v_a	$v_X = 5$	$v_X = 6$	$v_X = 7$	$v_X = 8$	$v_X = 9$
0	0.000872	0.000011	0.000000	0.000000	0.000000
1	0.049663	0.003688	0.000034	0.000001	0.000000
2	0.306350	0.102076	0.008669	0.000037	0.000006
3	0.080037	0.341575	0.163564	0.014735	0.000002
4	0.125146	0.011508	0.333349	0.226216	0.018747
5	0.009743	0.117118	0.001342	0.308178	0.279562
6	0.015218	0.047045	0.074435	0.017065	0.295899
7	0.048846	0.000367	0.070460	0.032564	0.030896
8	0.050905	0.014863	0.016649	0.066919	0.009550
9	0.031797	0.033137	0.000066	0.035926	0.045373
10	0.014359	0.035790	0.009645	0.007281	0.041817
11	0.004013	0.026111	0.018761	0.000008	0.019251
12	0.000450	0.016033	0.020658	0.003276	0.005243
13	0.000029	0.008179	0.016130	0.006126	0.000545
14	0.000256	0.003391	0.009187	0.005172	0.000005

Therefore, the numerical procedures and their precisions have been tested for various molecules [16], showing good agreement with the literature. For the states of interest in this work, the results obtained for the eigenvalues of $X^1\Sigma_g^+$ and $a^3\Sigma_g^+$ of H_2 are in agreement with those in [9,10] using the same potential curves. The transition probabilities and lifetimes for H_2 and D_2 in the $a^3\Sigma_g^+$ state, calculated using the method presented here, are given in table 3 for 15 vibrational levels. For the first four levels, the lifetimes for hydrogen are smaller than for deuterium, decreasing

Table 2. Franck–Condon factors for the transition $a^3\Sigma_g^+ \leftarrow X^1\Sigma_g^+$ for D_2. Tables of the Franck–Condon factors for all isotopes of the hydrogen molecule are available in ASCII format—click here.

v_a	$v_X = 0$	$v_X = 1$	$v_X = 2$	$v_X = 3$	$v_X = 4$
0	0.108257	0.298620	0.327221	0.190080	0.062625
1	0.188915	0.157012	0.000002	0.159953	0.277938
2	0.199845	0.018354	0.099958	0.097950	0.010659
3	0.165612	0.006621	0.111378	0.000648	0.127990
4	0.120075	0.046549	0.042331	0.057905	0.042065
5	0.080786	0.077652	0.002509	0.080607	0.001280
6	0.051839	0.085726	0.006100	0.047909	0.037956
7	0.032507	0.078196	0.027135	0.012860	0.059858
8	0.019925	0.063428	0.045205	0.000072	0.045982
9	0.012064	0.047696	0.052791	0.005503	0.020943
10	0.007460	0.035115	0.052860	0.017456	0.004534
11	0.004587	0.024982	0.047461	0.028081	0.000018
12	0.002772	0.017038	0.038718	0.033012	0.003549
13	0.001772	0.012062	0.031615	0.034860	0.009958
14	0.001117	0.008302	0.024471	0.032796	0.015648
v_a	$v_X = 5$	$v_X = 6$	$v_X = 7$	$v_X = 8$	$v_X = 9$
0	0.011857	0.001246	0.000063	0.000001	0.000000
1	0.164334	0.045517	0.006048	0.000336	0.000004
2	0.212414	0.244896	0.098474	0.016435	0.000971
3	0.022566	0.096230	0.272651	0.161187	0.033070
4	0.055162	0.090000	0.017082	0.247372	0.222577
5	0.086092	0.002709	0.116833	0.001309	0.190519
6	0.021323	0.064464	0.013004	0.090792	0.028114
7	0.001217	0.058005	0.019440	0.050287	0.045458
8	0.025589	0.012717	0.057553	0.000024	0.071733
9	0.043506	0.000677	0.039959	0.028258	0.012343
10	0.040766	0.015811	0.009572	0.046344	0.004225
11	0.025792	0.030980	0.000121	0.030285	0.029101
12	0.010882	0.032715	0.008352	0.008485	0.035836
13	0.002562	0.026358	0.019346	0.000111	0.024441
14	0.000006	0.016266	0.024277	0.003107	0.009197

with increasing quantum number in very good agreement with [5]. The small deviations are due to different potential curves used in the calculations. In addition, the results from [7] and [8] are included in table 3. The agreement between the data presented here and the data from [8] is excellent for all vibrational levels. The deviations of [7] for higher vibrational levels are due to the fact that the $A_{v_a,\lambda}$ values there were calculated only for $\lambda > 160$ nm. Therefore an extrapolation for $v_a = 3$–6 was necessary. The results presented here should be more accurate,

Table 3. Calculated integral transition probabilities A_{v_a} and radiative lifetimes τ_{v_a} for H_2 and D_2 (pw = present work) in comparison with literature. The calculated values for all isotopes of the hydrogen molecule are available in ASCII format—click here.

v_a	A_{v_a} (10^7 s^{-1})	τ_{v_a} (10^{-8} s)			A_{v_a} (10^7 s^{-1})	τ_{v_a} (10^{-8} s)	
	H₂				**D₂**		
	pw	pw	[5]	[8]	[7]	pw	pw	[5]
0	8.60	1.16	1.19	1.16	1.24	8.37	1.19	1.19
1	9.82	1.02	1.10	1.02	1.15	9.28	1.08	1.12
2	10.9	0.917	1.01	0.917	1.03	10.1	0.989	1.12
3	11.9	0.841	0.97	0.840	0.929	10.9	0.919	1.02
4	12.8	0.782		0.781	0.864	11.6	0.865	
5	13.7	0.732		0.730	0.807	12.2	0.818	
6	14.6	0.687		0.690	0.763	12.9	0.778	
7	15.6	0.642		0.641		13.5	0.742	
8	16.7	0.599		0.595		14.1	0.709	
9	18.2	0.551		0.549		14.8	0.677	
10	20.1	0.499		0.498		15.5	0.646	
11	22.8	0.439		0.439		16.2	0.616	
12	27.0	0.370		0.372		17.2	0.581	
13	32.7	0.306		0.299		18.3	0.547	
14	45.0	0.222		0.223		19.6	0.511	

especially for the repulsive state, because the calculations are based on precise potential curves, taking into account the full wavelength range $\lambda > 120$ nm with a very high energy resolution.

Shape and absolute value of the calculated continuum intensity vary with n_{v_X} and, via the rate coefficient for excitation from $X^1\Sigma_g^+$ to $a^3\Sigma_g^+$, with T_e, respectively. For the ground state $X^1\Sigma_g^+$, a thermal population with a vibrational temperature T_{vib} was adopted. The spectrum is sensitive to the population of the four lowest vibrational levels in $X^1\Sigma_g^+$, and an assignment of a vibrational temperature can be made. For hydrogen, the spectral photon emission coefficients for $0 < T_{vib} < 9000$ K and $T_e = 3$ eV are shown in figure 2 together with the spectral transition probabilities $A_{v_a,\lambda}$ for $v_a = 0$, 1 and 2. The most sensitive part of the continuum radiation is in the wavelength range 170–220 nm, which is thus particularly suitable for diagnostics. Around 190 nm, one can get a sensitive correlation of the intensity with T_{vib}. Difficulties may arise from the onset of the Lyman bands $B^1\Sigma_u^+ \to X^1\Sigma_g^+$ in this wavelength range, and perturbations in the population of the vibrational states in $a^3\Sigma_g^+$.

In figure 3, the vibrational populations in the $a^3\Sigma_g^+$ state are calculated for H_2 and D_2 for an electron temperature of 3.4 eV and different ground state vibrational temperatures. An increase of $T_{vib}(X)$ leads to higher vibrational level population in $a^3\Sigma_g^+$ until they approach a Boltzmann-like distribution. This can be seen in figure 3 for both isotopes. In the appropriate range, the vibrational temperature in the upper state can be correlated with a vibrational temperature in the ground state. For $T_{vib}(X) = 6000$ K the resulting $T_{vib}(a)$ is about 9000 K for H_2 and D_2.

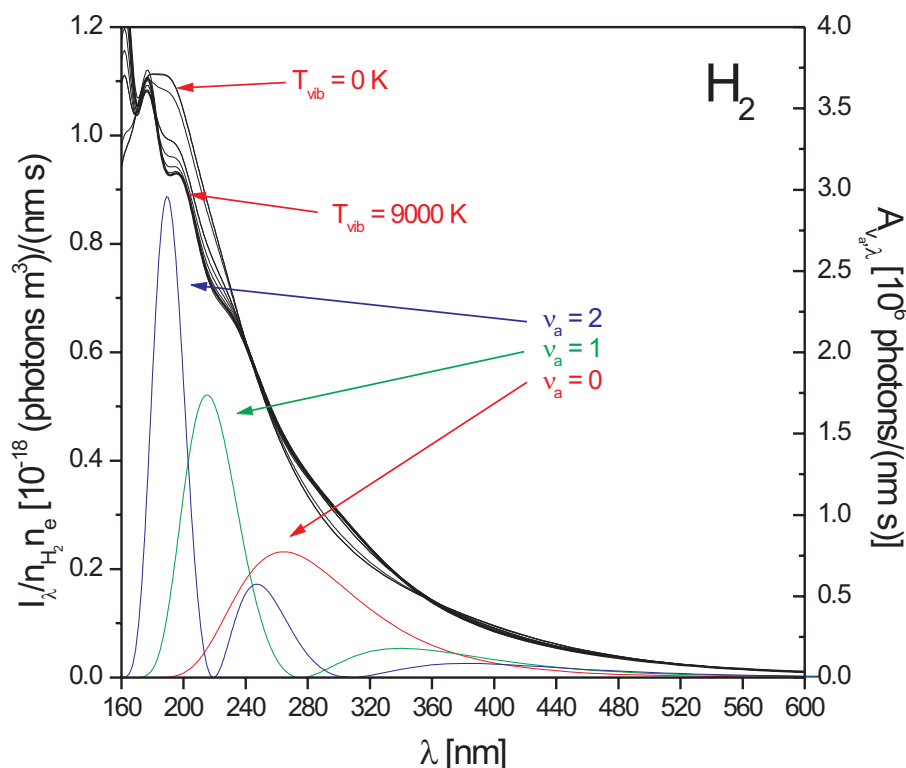Institute *of* **Physics** Φ DEUTSCHE PHYSIKALISCHE GESELLSCHAFT

Figure 2. Spectral photon emission rate coefficients $I_\lambda/n_{H_2}n_e$ of H_2 for $T_e = 3$ eV and ground state vibrational temperatures of $0 < T_{vib} < 9000$ K (left-hand scale) are shown together with the spectral transition probabilities $A_{v_a,\lambda}(\lambda)$ for the lowest three vibrational levels in $a^3\Sigma_g^+$ (right-hand scale). Tables of the $A_{v_a,\lambda}(\lambda)$ for all isotopes of the hydrogen molecule are available in ASCII format—click here.

3. Experiment

Low-pressure ECR (electron cyclotron resonance heated) plasmas were investigated at 2.45 GHz frequency, 100 W input power and a resonant magnetic field strength of 0.0875 T. The field was produced by two rows of permanent magnets of 1 T each at the surface. The magnets were located outside the vacuum vessel in the base plate, resulting in a region of resonance approximately 1 cm above the plate. Here, the plasmas are preferentially heated, and diffuse into the vessel volume (detailed information in [17]). The pressure range was 2–20 Pa, measured with a BARATRON pressure gauge.

For analysis of the plasma radiation, two spectrometers were used, which were located on opposite sides of the vessel and aligned on the same line-of-sight. The visible range was investigated by a 1 m SPEX spectrometer with a 2D CCD camera. For the UV/VUV range, a differentially pumped 1 m McPherson spectrometer with a 'solar blind' photomultiplier was mounted. Both spectrometers had a spectral resolution of about 55 pm and were calibrated by means of a tungsten ribbon lamp (OSRAM WI17/G) and a deuterium lamp (LOT Oriel type G.03). The tungsten ribbon lamp provided absolute calibration in the wavelength range 350–900 nm, which was extended to shorter wavelengths ($\lambda_{min} = 250$ nm) by means of the
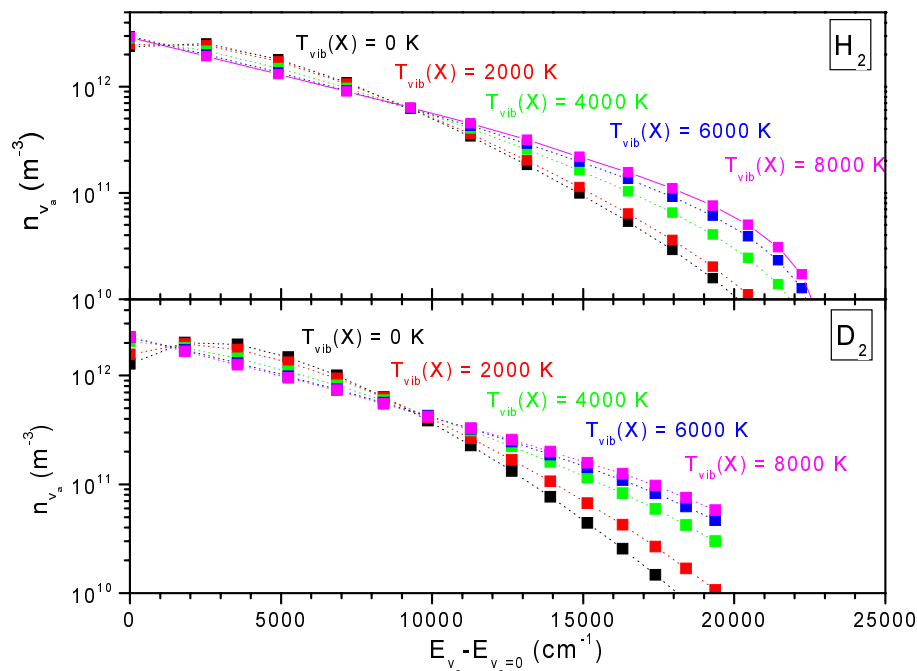
Figure 3. Calculated vibrational populations of H_2 and D_2 in the $a^3\Sigma_g^+$ state, depending on the ground state vibrational temperature for an electron temperature of 3.4 eV.

deuterium lamp with an overlap from 300 to 400 nm. The relative UV/VUV system response was determined by means of the deuterium lamp in the range 190–300 nm. For this purpose, the lamp was mounted in the vacuum vessel, thus avoiding oxygen absorption bands. The absolute sensitivity was obtained by cross-calibration using helium lines at $\lambda = 294.51$, 282.91, 276.38 and 272.32 nm in helium plasmas, which could be measured by both spectrometers. Using the branching ratio method for the Lyman–Birge–Hopfield system of N_2 plasmas [18], the calibration could be extended to shorter wavelengths. The accuracy of the calibration in the continuum range is expected to be better than 10%. A quartz plate was put into the optical path to eliminate the second-order Lyman and Werner bands in the range of the continuum radiation.

For the investigations described, hydrogen–helium and deuterium–helium plasmas were generated in various mixtures and at different pressures. All the plasmas were well characterized [4, 17] by various diagnostic methods. From microwave interferometry, a value of 9×10^{16} m^{-3} was derived for the electron density. Depending on pressure, the ionization degree was $\approx 10^{-4}$. Initially, the electron energy distribution function was assumed to be Maxwellian, an approximation which will be examined later in this paper. The gas temperatures, derived from the rotational temperatures of N_2 bands, were 450 K, typical for these types of plasma. For these measurements, a small amount of nitrogen was added. Rotational temperatures of hydrogen molecular bands are not well correlated with the gas temperature.

For a comparison of T_{vib} results, the diagonal Fulcher band emission from 590–650 nm $(v_d, v_a = 0$–3) was recorded simultaneously with the continuum radiation. Vibrational populations in the ground state, characterized by T_{vib} and derived from the Fulcher radiation, were found to range from 3200 K to 6800 K for H_2, and from 2600 K to 4000 K for D_2, depending on molecular density, pressure and electron temperature [4].

Electron temperatures of the investigated plasmas were determined from absolute measurements of the helium 728 nm line. The actual T_e values are of lesser significance, but they constitute the link to interpreting the absolute intensities of the hydrogen molecular continua and their underlying excitation rate coefficients. In short, the rate coefficients are just being compared with the helium excitation function. The quality of the helium data is therefore of high importance. The emission rate coefficients for the He 728 nm line were originally taken from Fujimoto's collisional radiative model [19], which takes into account the population of metastable states and the optical thickness of resonance lines. Both have been adjusted to the experimental data of the ECR plasmas [17]. However, He excitation cross-sections have recently been reviewed and corrected by highly accurate theoretical calculations [20]. Subsequently, Fujimoto has adopted these improvements into his program [21]. As a consequence, the excitation function for the particular transition used here, increased greatly: by a factor of four. This is mainly due to the increase of the direct excitation rate coefficient which is different by a factor of ten. In comparison to earlier analyses, measured temperatures are now lower, i.e. 2–4.5 eV depending on gas mixture and pressure. Even more important is the fact that a much better consistency of different spectroscopic criteria is now being observed and that many peculiar discrepancies found in the past are now explained.

4. Results and discussion

The ground state vibrational population, T_{vib}, was varied in the calculations until the best approximation to the shape of the measured continuum radiation was obtained. Wavelengths higher than 210 nm were given more weight. Figure 4 shows an example for measured and calculated spectra in plasmas with 8.8% H_2 or 10% D_2 in He at $p = 4$ Pa. Using $T_{vib} = 5500$ K for H_2 and $T_{vib} = 4000$ K for D_2, the agreement is very good in the wavelength range 210–300 nm. The sensitivity is estimated to be 500 K for lower T_{vib} increasing to 1000 K for higher T_{vib}. For the ground state, the population up to $v_X = 9$ was considered, and for the excited state, the population up to $v_a = 14$, with the assumption of corona equilibrium. It turns out that the population of the upper state is dominated by the population of the first four levels of the ground state. Therefore, a temperature can be assigned to these levels and the influence of higher levels could actually be neglected. The deviation in shape at lower wavelengths is about 15% of the radiation and may have various causes: the radiation of the Lyman bands is ten times higher than the continuum radiation, the maximum being at 162 nm. In addition, the Lyman band continuum caused by transition of the $v_B = 9$ level of the $B^1\Sigma_u^+$ state into the dissociation limit, is centred at 157.5 nm and 162.5 nm [22]. Both contribute to the radiation near 170 nm. Therefore, the measurements show an increase instead of a decrease. In this wavelength region, calibration or measurements may also be affected by water or oxygen absorption in the system. Lower radiation than predicted by the calculations is particularly noticeable at 200 nm for hydrogen plasmas. An analysis on the basis of single upper state vibrational levels demonstrates that this peak is correlated with radiation from $v_a = 2$.

According to the Franck–Condon factors, the $v_a = 2$ level of the $a^3\Sigma_g^+$ state should be substantially populated, as can been seen in figure 3. On the other hand, a reduction of only 15% in the number of $v_a = 2$ leads to spectra almost identical to the measured ones (green curve in figure 4), which demonstrates the sensitivity of the method. A possible reason for the observed discrepancy may therefore be sought in additional de-excitation paths for $v_a = 2$, like heavy particle collisions. In particular, collisions with molecules in the metastable $c^3\Pi_u$, $v_c = 0$ state
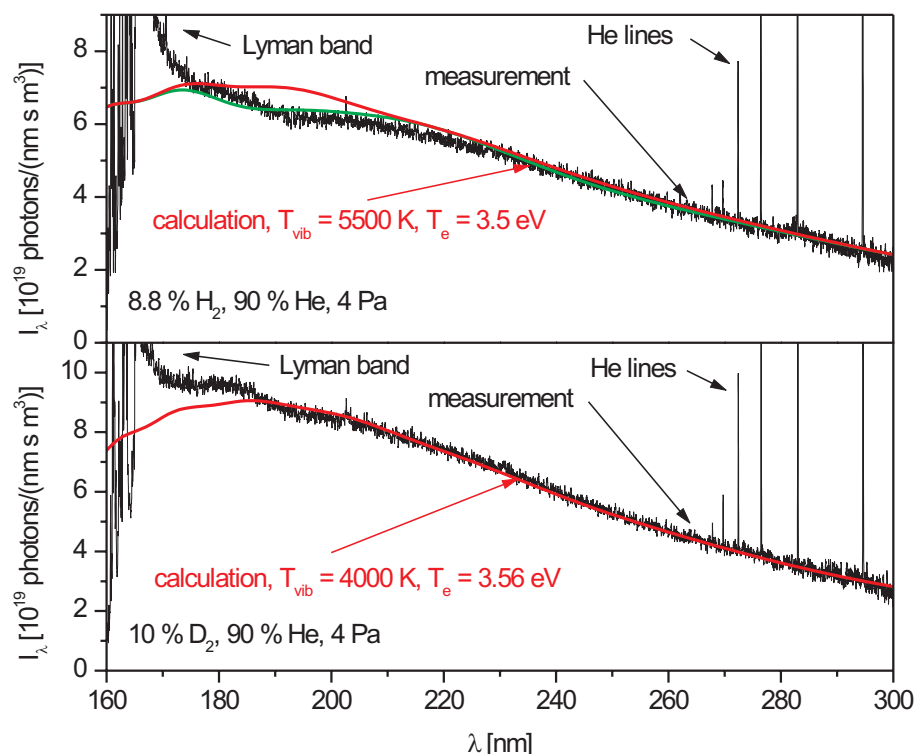
Figure 4. Examples of measurements of 8.8% H_2 (10% D_2) in He and calculations which give the best fit for $T_{vib} = 5500$ K (4000 K) and $T_e = 3.5$ eV (3.56 eV), respectively. Note the absolute scale. For H_2, the green curve has been obtained by reducing the population of $v_a = 2$ by 15% in the calculation.

can lead to redistribution processes. This level is only 0.05 eV lower than the $v_a = 0$ level. Vibrational levels higher than $v_c = 0$ can decay by spontaneous emission in the $a^3\Sigma_g^+$ level.

Results for the vibrational temperatures in the ground state of H_2 and D_2 (up to level $v_X = 3$) are given in figure 5 for $p = 4$ Pa. Because of the insensitivity of the method for temperatures below 1000 K, a temperature of 500 K has been assigned to these results. Depending on the concentration of molecules in helium plasmas, the population first decreases and then increases. There are many possible reasons for this behaviour, and two counteracting effects will be discussed here: with increasing molecule percentage, the depopulating heavy particle collisions (e.g. $H_2(v) + H_2 \rightarrow H_2(w) + H_2$; $w < v$) increase. On the other hand, wall collisions, which are also depopulating, decrease. A small effect of lesser importance is the variation of electron temperature, decreasing from 4 to 3 eV and leading to a smaller population by electron collisions. With respect to the isotopes, D_2 has a lower vibrational temperature, which actually reflects the same level population as in H_2 due to the smaller energy differences. For example, $T_{vib} = 4000$ K for H_2 is equivalent with $T_{vib} = 2900$ K for D_2, both having a relative population of 0.22 for $v = 1$ and 0.05 for $v = 2$ compared with the $v = 0$ level. These tendencies have also been obtained from measurements of the Fulcher band radiation and are discussed in more detail in [4]. The Fulcher band results for the 10% and 90% mixture in helium are included in figure 5. In this case, the accuracy of the method is 50 K at 1000 K and 250 K at 7000 K. The two methods are in good agreement, demonstrating the applicability of the continuum radiation as a diagnostic tool for vibrational population.
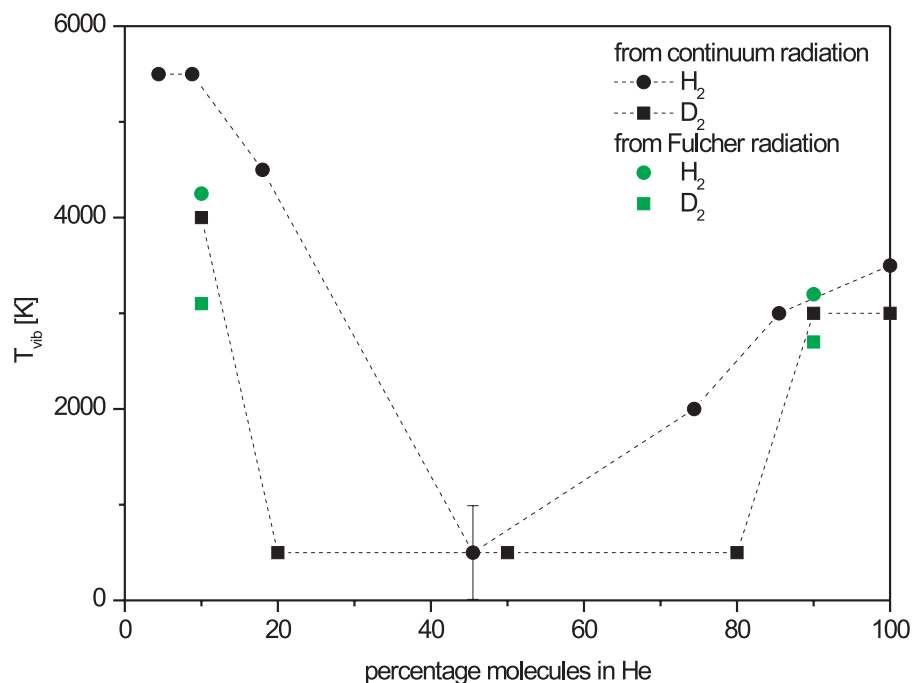
Institute *of* **Physics** Φ DEUTSCHE PHYSIKALISCHE GESELLSCHAFT

Figure 5. Vibrational temperatures depending on the concentration of hydrogen or deuterium in helium at 4 Pa, derived from the continuum spectra. Below 1000 K the method is insensitive and 500 K were assigned. For two concentrations, the results from Fulcher emissivity are included.

For determining the electron temperature from the continuum radiation, the measured absolute radiation was correlated with calculations using T_e as parameter and applying the adjusted T_{vib}. Integration of the fitted calculations over the whole wavelength range gives the total radiation of the transition. It turns out that, over the whole parameter range, nearly 50% of the radiation is either below 190 nm (30%) or above 300 nm (20%). These numbers are valid within 5% for both hydrogen and deuterium and can be applied generally for the determination of the total radiation, if only the part between 190–300 nm was measured. Using equations (1) and (3), T_e was evaluated by the emission rate coefficients for this transition. As mentioned before, the electron density was obtained from microwave interferometry and the molecular hydrogen density was obtained from Dalton's law. In the case of hydrogen, the demixing of the gases due to mass-dependent pumping was taken into account. The results for hydrogen and deuterium mixtures in helium are shown in figure 6.

Electron temperatures from the He line at 728 nm are also included in figure 6, which are in good agreement with the continuum results. The electron temperatures decrease with increasing number of molecules, being very similar in H_2 and D_2 plasmas. For the investigated plasmas, the spectroscopic method of determining the electron energy distribution function in the relevant energy range by adding small amounts of argon [23] was applied. In plasmas at 4 Pa, the He line and the Ar line at 696 nm give the same temperatures, which is an indication that the electron distribution function is Maxwellian. For higher pressures, the temperature derived from the Ar line is higher than the temperature from the He line, and the electron energies can be described by a distribution function which is between Maxwellian and Druyvensteyn shape. The good
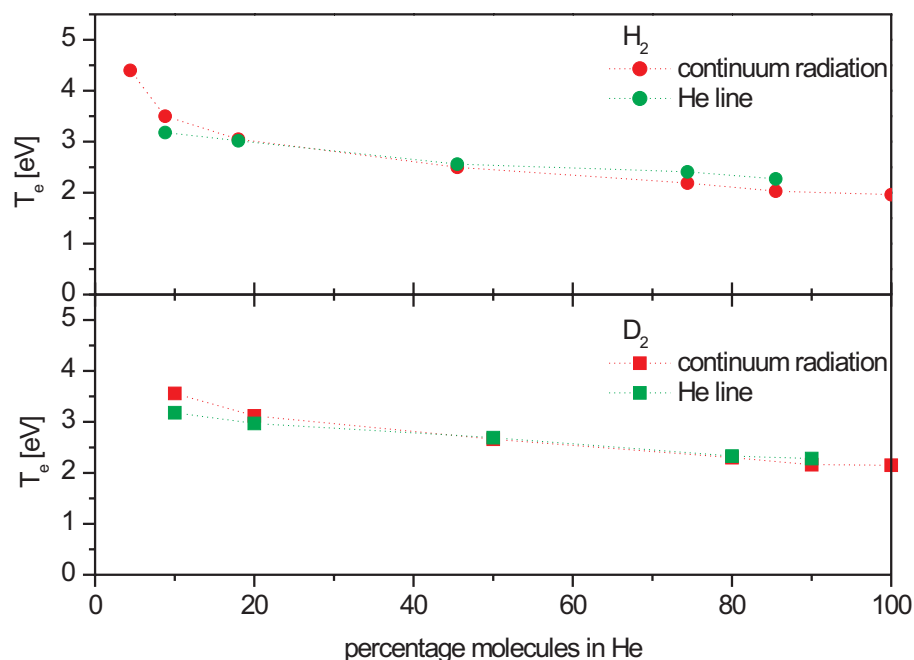
Figure 6. Electron temperatures derived from the continuum spectra in various H_2 and D_2 concentrations in helium plasmas at 4 Pa, compared with results from the radiation of the 728 nm He line.

agreement in the electron temperatures derived from the continuum and the He line in the case of a Maxwellian distribution function demonstrates the applicability of the cross-section from [11] in low-pressure plasmas. The lower cross-sections from [12] or [13] would result in higher T_e by 0.2 eV, which is outside the error range of the method.

5. Conclusions

A general procedure for calculating free and bound wave functions of diatomic molecules was implemented and applied to hydrogen and its isotopes. It yields Franck–Condon factors, transition probabilities and lifetimes, if the potential curves, the reduced masses and the electronic dipole transition moments are known. For a bound–bound ($a^3\Sigma_g^+ \leftarrow X^1\Sigma_g^+$) and a bound–free transition ($a^3\Sigma_g^+ \rightarrow b^3\Sigma_u^+$), a complete set of data with high accuracy for H_2, D_2, T_2, HD and DT has been presented. The continuum radiation of hydrogen and deuterium molecules in the wavelength range 190–300 nm was calculated on the basis of the electron excitation rate coefficient as a function of T_e, taking into account vibrational population in the ground state.

This allows comparison with measurements from plasma experiments on an absolute scale. The shape of the continuum is dominated by T_{vib}, whereas the absolute value results from T_e. The results show a variation in T_{vib} and T_e with concentration of hydrogen molecules, and the influence of the isotopes is apparent. The sensitivity to T_{vib} is sufficient. There is a good agreement with results from other spectroscopic techniques, thus establishing a diagnostic tool for T_{vib} and T_e in H_2 and D_2. The calculation of the spectra can easily be applied to other isotopes, because the program is only based on potential curves and reduced masses. An example of the variation of the spectra for isotopes is shown in figure 7. This may be of interest in the boundary layer of
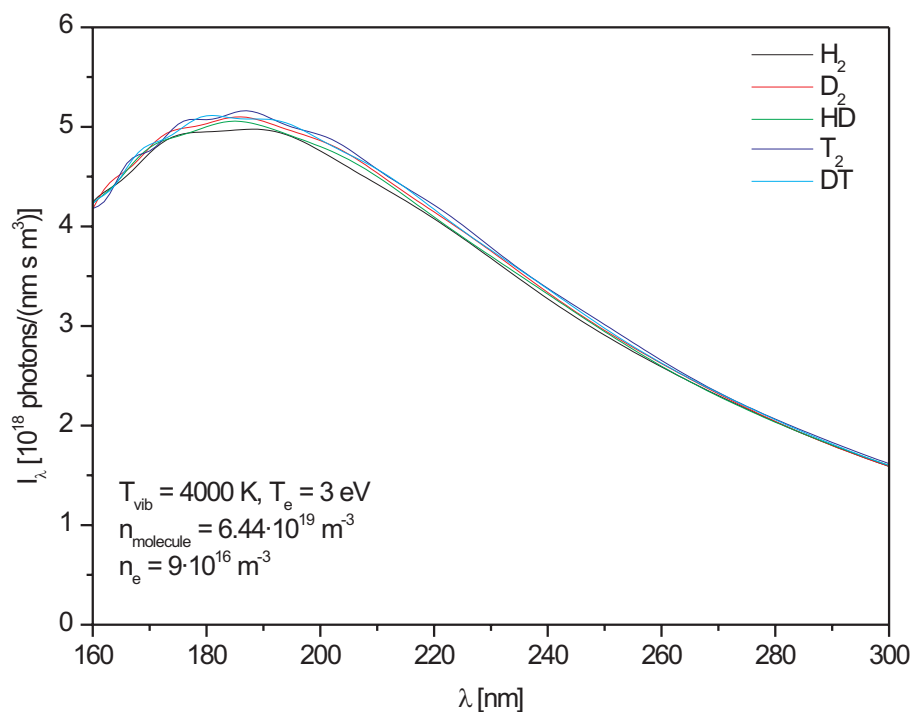
Institute *of* **Physics** Φ DEUTSCHE PHYSIKALISCHE GESELLSCHAFT

Figure 7. Calculated spectrum for $n_{\mathrm{molecule}} = 6.44 \times 10^{19}$ m^{-3}, $n_e = 9 \times 10^{16}$ m^{-3}, $T_{vib} = 4000$ K, $T_e = 3$ eV of the different isotopes.

fusion experiments, where T_e is small and molecules can exist. Here, the three isotopes exist together with the heteronuclear molecules HD or DT. HD radiation can be studied in laboratory experiments, whereas DT has to be taken from theory. Another field of application may be the prediction or control of the radiation of D$_2$ and H$_2$ lamps often used as calibration sources in the UV range. The measurements and calculations introduced represent a basis for further understanding of the molecular radiation and pertinent atomic processes.

References

[1] Otorbaev D K, de Graaf M J, van de Sanden M C M and Schram D C 1995 *Contr. Plasma Phys.* **35** 195
[2] Astashkevich S A, Käning M, Käning E, Kokina N V, Lavrov B P, Ohl A and Röpke J 1996 *J. Quant. Spectrosc. Radiat. Transfer* **56** 725
[3] Schulz–von der Gathen V and Döbele H F 1996 *Plasma Chem. Plasma Proc.* **16** 461
[4] Fantz U and Heger B 1998 *Plasma Phys. Control. Fusion* **40** 2023
[5] James H M and Coolidge A S 1939 *Phys. Rev.* **55** 184
[6] Doyle R O 1965 *PhD Thesis* Harvard University
[7] Lavrov B P, Melnikov A S, Käning M and Röpcke J 1999 *Phys. Rev.* E **59** 1
[8] Kwok T L , Gubermann S, Dalgarno A and Posen A 1986 *Phys. Rev.* A **34** 1962
[9] Kolos W and Wolniewicz L 1965 *J. Chem. Phys.* **43** 2429
[10] Kolos W and Wolniewicz L 1968 *J. Chem. Phys.* **48** 3672
[11] Lima M A P, Gibson T L, McKoy V and Huo W M 1988 *Phys. Rev.* A **38** 4527
[12] Chung S and Lin C C 1978 *Phys. Rev.* A **17** 1874
[13] Rescigno T N, McCurdy C W Jr, McKoy V and Bender C F 1976 *Phys. Rev.* A **13** 216

Institute *of* **Physics** Φ DEUTSCHE PHYSIKALISCHE GESELLSCHAFT

[14] Khakoo M A and Trajmar A 1986 *Phys. Rev.* A **34** 146

[15] Sawada K and Fujimoto T 1995 *J. Appl. Phys.* **78** 2913

[16] Schalk B 1998 *Diplomarbeit* Institut für Physik, Universität Augsburg

[17] Fantz U 1998 *Plasma Phys. Control. Fusion* **40** 1035

[18] Mumma M J 1972 *J. Opt. Soc. Am.* **62** 1459

[19] Fujimoto T 1979 *J. Quant. Spectrosc. Radiat. Transfer* **21** 439

[20] De Heer F J, Hoekstra R, Kingston A E and Summers H P 1992 *JET-P(92)09*

[21] Fujimoto T 1995 *private communication*

[22] Stephens T L and Dalgarno A 1972 *J. Quant. Spectrosc. Radiat. Transfer* **12** 569

[23] Behringer K and Fantz U 1994 *J. Phys. D: Appl. Phys.* **27** 2128